Proceedings of the Korean Nuclear Society Spring Meeting
Gyeongju, Korea, 2004

# Fuel Safety Analysis of the End Fitting Failure Accident for the CANFLEX-NU Fuel Loading into Wolsong1 NPP

**Yong-Deog Kim**

Korea Electric Power Research Institute
103-16 Munji-dong, Yusung-gu
Taejeon, Korea 305-380

## ABSTRACT

The fuel safety analysis of the end fitting failure accident is done for Wolsong1 Nuclear Power Plant(NPP) loaded with CANFLEX-NU fuel. The objective of the fuel safety analysis of the end fitting failure is to estimate the quantity and timing of fission product release from the fuel that is discharged to the fueling machine vault. Fission product inventories at the time of the accident in fuel bundles of the broken channel and the temperature transient of the fragments as well as the fission product releases due to oxidation are calculated by ELESTRESS and REDOU computer code respectively. Release from the fuel matrix is limited to 12 percent of the bound inventory in outer elements of bundle 7.

## 1. Introduction

An end fitting failure (EFF) in a single channel would result in behaviour similar to that of a small reactor header break with respect to the thermohydraulic response of the primary circuit and the containment building. However, this event differs from a small header break in that all the fuel bundles in the affected channel could be ejected into the fuelling machine vault. Therefore, unlike small header breaks, the focus is on the behaviour of the ejected fuel, as opposed to the primary circuit. In particular, the end fitting failure assessment concentrates on the release of fission products into containment due to the oxidation of ejected fuel. This assessment illustrates the important role of the radiation monitors in preventing a potentially large release of fission products outside the containment shortly after the event occurs.

### 2. CANFLEX-NU Fuel Description

The CANFLEX-NU (CANDU-FLEXIBLE-Natural Uranium) fuel bundle is a 43-element natural uranium design containing an array of fuel elements of two different diameters. Figure 1 shows a schematic diagram of a CANFLEX-NU bundle cross section. The larger (inner 8) elements have a fuel pellet diameter of 12.67 mm, and the smaller (outer 35) elements have a 10.73 mm fuel pellet diameter. Different element diameters and larger number of elements in CANFLEX-NU bundle design is well known to reduce the peak linear outer element power ratings by approximately 20% at the same overall

bundle power output (Alavi, 1995).

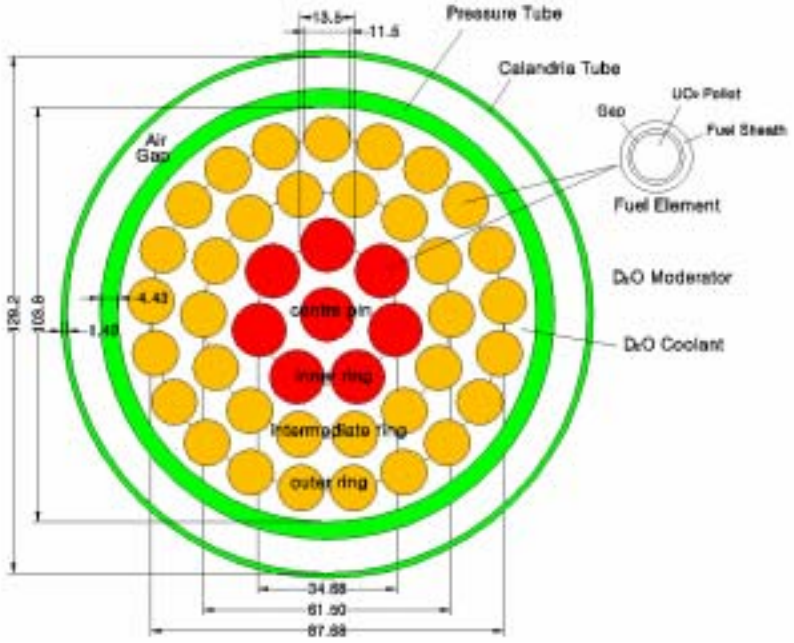


**Figure 1. Cross Section of the CANFLEX Fuel Channel**

## 3. Fuel Analysis Scope

For the estimates of fission product release, the burnups of the twelve bundles in the channel are assumed to be their respective burnups before the time the channel is about to be refuelled, less then the “limiting burnup”. The limiting burnup distribution is determined from the maximum bundle average burnup for each bundle location among the 380 channels as predicted in the time-average fuel management simulations. Generally, the maximum total inventories are expected to occur at the end-of-life (long-lived fission products), or about 10 to 20 MW.h/kg(U) after the plutonium peak (short-lived fission products). Table 1 gives the channel powers and bundle burnups considered in the assessment.

### 3.1 Calculation of the Temperature Transients for Fuel Fragments

Dropping a CANDU fuel bundle onto the vault floor is known to break the bundle into single elements or small clusters of elements. Some of the fuel elements which are ejected might break into several pieces. Few sheath failures have been observed in impact tests using irradiated and unirradiated fuel bundles (Reference 1).

To simplify the analysis, all fuel element sheaths in the affected channel are assumed to fail immediately at the time of the accident. Therefore, no detailed analysis of fuel sheath behaviour following the accident is required. Furthermore, the fuel element sheaths are assumed to be sufficiently damaged that the fuel pellets are ejected. Fuel pellets are assumed to break into fragments.

Table 1. Fuel Bundle and Element Power/Burnup Distributions in the O6_mod Channel

| Bundle Position | Bundle (kW, MWh/kg) | Outer Element (kW, MWh/kg) | Intermediate Element (kW, MWh/kg) | Inner Element (kW, MWh/kg) | Center Element (kW, MWh/kg) |
|---|---|---|---|---|---|
| 1 | 111.7/43.8 | 5.72/49.68 | 4.71/41.07 | 5.82/36.39 | 5.56/34.78 |
| 2 | 406.1/102.4 | 20.79/116.14 | 17.11/96.02 | 21.15/85.08 | 20.22/81.32 |
| 3 | 619.7/139.8 | 31.73/158.56 | 26.11/131.09 | 32.27/116.16 | 30.85/111.02 |
| 4 | 761.4/161.5 | 38.99/183.17 | 32.09/151.44 | 39.65/134.19 | 37.91/128.25 |
| 5 | 874.0/175.6 | 44.75/199.17 | 36.83/164.66 | 45.51/145.91 | 43.51/139.44 |
| 6 | 935.0/188.5 | 47.88/213.80 | 39.40/176.76 | 48.69/156.62 | 46.55/149.69 |
| 7 | 935.0/188.5 | 47.88/213.80 | 39.40/176.76 | 48.69/156.62 | 46.55/149.69 |
| 8 | 875.6/175.6 | 44.84/199.17 | 36.90/164.66 | 45.60/145.91 | 43.59/139.44 |
| 9 | 744.9/198.6 | 38.14/225.25 | 31.39/186.23 | 38.79/165.02 | 37.09/157.71 |
| 10 | 577.5/229.9 | 29.57/260.75 | 24.34/215.58 | 30.07/191.02 | 28.75/182.56 |
| 11 | 363.8/230.0 | 19.65/260.87 | 16.17/215.67 | 19.99/191.11 | 19.11/182.64 |
| 12 | 95.3/198.6 | 4.88/225.25 | 4.02/186.23 | 4.96/165.02 | 4.74/157.71 |

A survey of different fragment sizes is performed.. The temperature decreases faster for small fragment sizes than for larger ones. However, the surface/volume ratio, which limits fuel oxidation, is inversely proportional to the fragment size. All of the $UO_2$ pellets are conservatively assumed to be ejected from the sheaths and break into fragments of varying sizes, ranging from 1.0 mm to 7.64 mm (corresponding to an intact pellet). The fragments are assumed to be spherical. The REDOU code (References 2 and 3) simulates the temperature transient of the fragments as well as the fission product releases due to oxidation. The fragment temperatures are estimated by assuming that the fuel temperatures at the time of the accident are the volume-average fuel temperatures prior to the ejection, taken from the ELESTRES (References 4 and 5) simulations using the limiting power and burnup distributions.

The fragments cool by convective and radiative heat transfer to still air at 100°C, the temperature of saturated steam at atmospheric pressure. The minimum convective heat transfer coefficient for spheres is 5 $W/m^2.K$ for the range of fragment sizes and expected temperatures. The radiative heat transfer assumes an emissivity of 0.7, lower bound as given in MATPRO-11 (Reference 6). The fragments generate heat, which is assumed to be uniformly distributed. The heat generated due to oxidation is small compared to the assumed initial temperature and fission product decay heat generation. MATPRO-11 is also used to estimate the heat capacity of $UO_2$ at the different initial temperatures as shown in Table 2. Fission product releases are greater for higher fuel temperatures. Thus, to provide a margin for uncertainties, fuel temperatures have been over-estimated.

Table 2. Specific Heat Capacity of UO2 Used in REDOU Simulations (MATPRO 11 Correlation)

| Temperature (°C) | Specific Heat Capacity (W.s/kg. °C) |
|---|---|
| 0 – 400 | 298 |
| 400 – 800 | 317 |
| 800 – 1200 | 331 |
| 1200 – 1600 | 359 |
| 1600 – 1900 | 404 |

### 3.2 Determination of the Fission Product Releases From Fuel Fragments

An element from each ring of the 12 bundles in the 7.3 MW channel (O6_mod) is simulated using the ELESTRES code to estimate fission product inventories in each element in the channel at the time of the accident. The maximum total and the maximum gap inventories of each of the isotopes are obtained from each ELESTRES simulation. At the time of sheath failure (time zero), the gap inventory of all of the fuel elements in the channel is assumed to be released. The remaining fission product inventory is bound within the grains or on the grain boundaries of the fragments of $UO_2$. When a fuel pellet fractures into many small fragments, the surface area of exposed $UO_2$ increases. It is assumed that this increase in exposed surface area causes additional release of fission products which were previously on grain boundaries. The inventory of fission product isotopes on grain boundaries is obtained from the ELESTRES code simulations. The fraction of the grain boundary inventory released after fuel fragmentation is assumed to be equal to the ratio of exposed surface area to the total grain surface area in the pellet. The total grain surface area is calculated by assuming that the grains are spherical, half of diameter 200 ⌈m and half of diameter 15 ⌈m (double the initial grain size). The surface-to-volume (S/V) ratio of grains is thus calculated to be 215 $mm^{-1}$. The S/V ratio of the fragments is calculated from the assumed fragment sizes. For example, for 1 mm diameter spheres, the S/V ratio is 6 $mm^{-1}$, and therefore the fractional release from grain boundaries is approximately 0.03. The REDOU code is used to estimate the extent of fuel oxidation in air, and the resulting fractional release of bound iodine based on References 7 and 8. $UO_2$ oxidizes more slowly in steam or near-steam (95 percent) atmospheres than in air. Therefore, the rate of steaming from the coolant discharge into the vault affects the rate of fuel oxidation and timing of fission product releases from the fuel. However, releases into containment are based on continuous oxidation only.

Enhancement of diffusional fission product releases from fuel occurs upon conversion of $UO_2$ to $U_3O_8$ (Reference 7). Above 900°C, oxidation to $U_3O_8$ will occur only after an incubation period and the rate of oxidation is temperature-dependent. This incubation period may be represented as the time required to reach a critical thickness of $U_4O_9$, before which oxidation to $U_3O_8$ does not occur. The incubation time is not accounted for in the calculation. A sample in air at 500°C was reported to be 100% oxidized to $U_3O_8$ after approximately 50 minutes. Samples in air at 400, 600 and 700°C were reported to oxidize at slower rate. To ensure that the oxidation rate is overestimated, 10% of the remaining $UO_2$ is assumed to oxidize per minute at temperatures below 900°C. A consequence of this assumption is that, regardless of the conditions, all fragments are completely oxidized after 600 s or less. The total fission product release from the oxidized fuel is a function of the temperature of the oxidized fuel as given in Table 3and the

oxidized fraction of uranium dioxide.

Table 3. Iodine Release Constant* as a Function of Temperature

| Temperature (°C) | Release Constant (%) |
|---|---|
| 600 | 4.0 |
| 700 | 7.6 |
| 800 | 14.5 |
| 900 | 27.6 |
| 1000 | 52.5 |
| 1100 | 100.0 |

* Release constant, $Kr=10^{0.0028T-3.08}$, where T is temperature in °C

Fractional release of iodines = Kr x (oxidized fraction of uranium dioxide)

Above 1100°C, 100% of the iodine in the oxidized $UO_2$ is released. At 600°C, the total release is approximately 4%. There is no data on iodine release at temperatures below 600°C. Therefore below 600°C the fractional release is held constant at 4%. The fractional release transient from each element is then multiplied by the bound inventory of iodine for that element to obtain the iodine activity transient. These are then summed up over all of the elements in the O6_mod channel. The grain bound inventories of noble gases are assumed to be instantly released at the time of accident.

## 3. Analysis Results

For the 7.3MW channel with the two 935kW bundles (O6_mod), the initial and final temperature of fragments used to perform the oxidation analysis following ejection if the bundles are given in Table 4. The temperature of fuel fragments from the outer elements of bundle 7 is 944 °C at time zero and decreases rapidly to 518 °C by 23 seconds. Therefore, most of fission product releases occur during the early part of the temperature transient. There are three different types of temperature transient as summarized in Table 5.

Table 6 gives the estimated fission product inventory and distribution in channel O6_mod. The fission product release is determined by fuel temperature and extent of oxidation. Using the temperature transient, the extent of oxidation of fuel pellet pieces from the O6_mod channel is obtained. By the end of the simulations (600 s), all fragments from the channel are completely oxidized and release rate goes to zero, regardless of fragment sizes and initial temperatures. The rate of oxidation affects the rate of release, but not total release. For the O6_mod channel, a series of iodine release transients are estimated by using the various assumed initial $UO_2$ fragment sizes. Critical fragment sizes are defined as the ones which give the highest releases. I-131 releases and release frations for iodine isotopes are given in Table 7. Release from the fuel matrix is limited to 12 percent of the bound inventory in outer elements of bundle 7. At lower initial temperature, releases are only 4 to 5 percent of bound inventory and are somewhat

independent of the extent of oxidation.

The entire channel inventories of noble gases are assumed to be released at the beginning of the transient (Table 8).

Table 4. Fuel Bundle and Element Power/Burnup Distributions in the O6_mod Channel

| Bundle Position | Outer Element | Intermediate Element | Inner Element | Center Element |
|---|---|---|---|---|
| 1 | 325 - 119 | 316 - 116 | 325 - 114 | 323 - 113 |
| 2 | 470 - 162 | 436 - 152 | 470 - 147 | 461 - 145 |
| 3 | 591 - 443 | 530 - 411 | 594 - 391 | 578 - 384 |
| 4 | 713 - 480 | 602 - 445 | 702 - 425 | 671 - 417 |
| 5 | 863 - 509 | 670 - 470 | 862 - 450 | 823 - 441 |
| 6 | 929 - 519 | 712 - 482 | 924 - 460 | 872 – 454 |
| 7 | 944 - 518 | 722 - 482 | 946 - 460 | 892 - 455 |
| 8 | 898 - 511 | 700 - 470 | 914 - 448 | 849 - 442 |
| 9 | 788 – 476 | 627 - 442 | 757 - 421 | 709 - 414 |
| 10 | 599 - 431 | 544 - 399 | 603 - 381 | 589 - 374 |
| 11 | 493 - 159 | 461 - 150 | 495 - 145 | 487 - 143 |
| 12 | 357 - 116 | 350 - 114 | 358 - 112 | 356 - 112 |

Table 5. Release Transient Types for the Fuel Elements in the O6_mod Channel

| | Element Position | Element Power (kW/m) | Critical Fragment Size (mm) | Initial Temperature (°C) |
|---|---|---|---|---|
| Type 1 | BP1 (Outer, Inter, Inner, Center)<br>BP12 (Outer, Inter, Inner, Center) | 4.02 – 5.82 | 1.00 | 316 – 358 |
| Type 2 | BP3 (Outer, Inter, Inner, Center)<br>BP4 (Outer, Inter, Inner, Center)<br>BP5 (Outer, Inter, Inner, Center)<br>BP6 (Outer, Inter, Inner, Center)<br>BP7 (Outer, Inter, Inner, Center)<br>BP8 (Outer, Inter, Inner, Center)<br>BP9 (Outer, Inter, Inner, Center)<br>BP10 (Outer, Inter, Inner, Center) | 24.34 – 48.69 | 7.64 | 530 - 946 |
| Type 3 | BP2 (Outer, Inter, Inner, Center)<br>BP11 (Outer, Inter, Inner, Center) | 16.17 – 21.15 | 1.00 | 436 - 495 |

Table 6. Inventory Distributions of Iodine and Noble Gas Isotopes in Channel O6_mod at the time of the Accident (End Fitting Failure)

| Isotope | Total Inventory (TBq) | Gap Inventory (TBq) | Grain Boundary Inventory (TBq) | Grain Bound Inventory (TBq) |
|---|---|---|---|---|
| I-131 | 191.77 | 1.57 | 20.41 | 169.8 |
| I-132 | 7697.71 | 13.83 | 936.28 | 6747.6 |
| I-133 | 12016.68 | 25.64 | 1480.87 | 10510.16 |
| I-134 | 18779.52 | 9.56 | 2192.24 | 16577.71 |
| I-135 | 21015.21 | 2.21 | 2419.27 | 18593.72 |
| I-137 | 17633.78 | 5.08 | 2042.87 | 15585.83 |
| Kr-83m | 9305.94 | 0.16 | 1068.02 | 8237.76 |
| Kr-85m | 1453.18 | 0.08 | 167.02 | 1286.08 |
| Kr-85 | 3549.11 | 0.32 | 408.36 | 3140.44 |
| Kr-87 | 22.86 | 0.14 | 2.44 | 20.28 |
| Kr-88 | 6902.61 | 0.33 | 793.04 | 6109.23 |
| Kr-89 | 9753.07 | 0.7 | 1121.44 | 8630.93 |
| Xe-133m | 12659.43 | 0.12 | 1452.51 | 11206.79 |
| Xe-133 | 530.88 | 0.17 | 61.56 | 469.16 |
| Xe-135m | 17219.16 | 20.48 | 2055.77 | 15142.91 |
| Xe-135 | 3018.14 | 0.06 | 346.44 | 2671.64 |
| Xe-137 | 2012.09 | 0.84 | 234.13 | 1777.12 |
| Xe-138 | 17102.8 | 0.18 | 1962.4 | 15140.22 |

Table 7. I-131 Releases (TBq) and Release Fractions from the Grain Boundary and Bound Inventory of the Fuel Elements in the O6_mod Channel

| Bundle Position | Outer Ring | Intermediate Ring | Inner Ring | Center Ring |
|---|---|---|---|---|
| 1 | 2.2 (0.04) | 1.2 (0.04) | 0.7 (0.04) | 0.1 (0.04) |
| 2 | 8.7 (0.04) | 4.7 (0.04) | 2.9 (0.04) | 0.4 (0.04) |
| 3 | 13.6 (0.04) | 7.4 (0.04) | 4.5 (0.04) | 0.6 (0.04) |
| 4 | 20.9 (0.05) | 9.1 (0.04) | 5.5 (0.04) | 0.7 (0.04) |
| 5 | 31.2 (0.07) | 12.2 (0.05) | 9.1 (0.06) | 1.0 (0.05) |
| 6 | 49.1 (0.11) | 12.2 (0.05) | 12.2 (0.08) | 1.2 (0.06) |
| 7 | 53.5 (0.12) | 12.2 (0.05) | 13.7 (0.09) | 1.2 (0.06) |
| 8 | 84.7 (0.09) | 12.2 (0.05) | 10.7 (0.07) | 1.0 (0.05) |
| 9 | 21.5 (0.05) | 9.3 (0.04) | 5.6 (0.04) | 0.8 (0.04) |
| 10 | 14.7 (0.04) | 7.9 (0.04) | 4.8 (0.04) | 0.6 (0.04) |
| 11 | 11.0 (0.04) | 5.9 (0.04) | 3.5 (0.04) | 0.5 (0.04) |
| 12 | 4.9 (0.04) | 2.5 (0.04) | 1.4 (0.04) | 0.2 (0.04) |

Table 8. Inventory Releases of Noble Gas Isotopes at the time of the Accident of End Fitting Failure (Total Inventories in the O6_mod Channel)

| Isotope | Half Life (s) | Inventory Release (TBq) |
|---|---|---|
| Kr-83m | 6.7E+03 | 9305.94 |
| Kr-85m | 1.61E+04 | 1453.18 |
| Kr-85 | 3.38E+08 | 3549.11 |
| Kr-87 | 4.56E+03 | 22.86 |
| Kr-88 | 1.01E+04 | 6902.61 |
| Kr-89 | 1.90E+02 | 9753.07 |
| Xe-133m | 1.93E+05 | 12659.43 |
| Xe-133 | 4.57E+05 | 530.88 |
| Xe-135m | 9.18E+02 | 17219.16 |
| Xe-135 | 3.30E+04 | 3018.14 |
| Xe-137 | 2.29E+02 | 2012.09 |
| Xe-138 | 8.52E+02 | 17102.8 |

## 5. Summary and Conclusions

For a postulated end fitting failure, adequate trip coverage is provided by the two shutdown systems and the emergency core cooling system refills the heat transport system, such that there

is no fuel heat up in the intact channels. This satisfies the criteria for prevention of systematic fuel failures and maintenance of fuel channel integrity. Releases of radionuclides from the fuel bundles ejected from the failed end fitting and subsequently from containment due to leakage are such that the dose limits for the individual and the population are satisfied.

## 6. References


1. P.M. Matthew et al., “Disassembly Behaviour of CANDU Bundles Under Impact”, Proceedings of the Third International Conference on CANDU Fuel, Chalk River, ISBN 0-919784-25-9, 1992 October.
.2. R. Aboud, “REDOU Version 1.0: Fractional Fission Product Releases Due to Oxidation of Uranium Dioxide – Program Description, User’s Manual and Validation”, TTR-378, Volume 1, 1992 January.
3. 15.2.1.5.A-10. R. Aboud, “REDOU Version 1.0: Fractional Fission Product Releases Due to Oxidation of Uranium Dioxide – Programmers Guide and Source Listing”, TTR-378, Volume 2, 1991 December.
4. M. Tayal, “Modelling CANDU Fuel Under Normal Operating Conditions: ELESTRES Code Description”, AECL-9331, 1987 February.
5. M. Tayal, “ELESTRES” Performance of Nuclear Fuel, Circumferential Ridgingand Multiaxial Elastic-Plastic Stresses in Sheaths”, International Conference on CANDU Fuel, Chalk River, Ontario, 1986 October.
6. D.L. Hagrman and G.A. Reymann (eds.), “MATPRO Version 11-A Handbook of Materials Properties for Use in the Analysis of Light Water Reactor Fuel Rod Behaviour”, TREE-NUREG-1280, 1979 February.
7. D.S. Cox, F. Iglesias, et al., “Oxidation of $UO_2$ in Air and Steam with Relevance to Fission Product Releases”, Presented at American Chemical Society Symposium on Chemical Phenomena Associated with Radioactivity Releases During Nuclear Plant Accidents, Anaheim (California), 1986 April.
8. 15.2.1.5.A-16. F. Iglesias, D.S. Cox, and C.E.L. Hunt and N.A. Keller, “$UO_2$ Oxidation and Fission Product Release”, Presented at USNRC Severe Fuel Damage Review Meeting, Oak Ridge, USA, 1986 April.